Spontaneous-relaxation-rate suppression in cavities with $\mathcal{PT}$ symmetry

Alireza Akbarzadeh,[1] Maria Kafesaki,[2,3] Eleftherios N. Economou,[2] Costas M. Soukoulis,[2,4] and J. A. Crosse[5,6,*]

[1]*Department of Engineering Physics, Polytechnique Montréal, Montréal, Canada QC H3T 1J4*

[2]*Foundation for Research & Technology-Hellas, Heraklion, Crete 71110, Greece*

[3]*Department of Materials Science and Technology, University of Crete, Heraklion 71003, Greece*

[4]*Ames Laboratory and Department of Physics and Astronomy, Iowa State University, Ames, Iowa 50011, USA*

[5]*New York University Shanghai, 1555 Century Ave, Pudong, Shanghai 200122, China*

[6]*NYU-ECNU Institute of Physics at NYU Shanghai, 3663 Zhongshan Road North, Shanghai 200062, China*

(Received 19 September 2018; published 27 March 2019)

We compute the spontaneous relaxation rate of a two-level atom in a planar cavity with parity ($\mathcal{P}$) and parity-time ($\mathcal{PT}$) symmetry. We find that at the center of a $\mathcal{PT}$-symmetric cavity the evanescent contribution to the relaxation rate is greatly suppressed. As this is the dominant relaxation pathway for cavities smaller than the transition wavelength, $\mathcal{PT}$-symmetric microcavities are able to suppress the spontaneous relaxation rate dramatically and, in some cases, reduce it to below the free-space level. The ability to reduce the relaxation rate and lengthen the excited-state lifetime has many applications in quantum control and can, for example, be used to increase atomic trapping times, improve photonic storage, and help maintain the coherence of atomic qubits.

DOI: 10.1103/PhysRevA.99.033853

I. INTRODUCTION

In the conventional formulation of quantum mechanics, Hermiticity was considered to be a necessary condition for a Hamiltonian operator to exhibit a real spectrum of eigenvalues. Bender *et al.* [1–3] showed that a non-Hermitian Hamiltonian $\hat{H}$ can possess real eigenvalues in a certain region of parameter space if $\mathcal{PT}$ symmetry is preserved, i.e., $[\hat{H}, \hat{\mathcal{P}}\hat{\mathcal{T}}] = 0$. A notable feature of these systems is the $\mathcal{PT}$-phase transition where, at some threshold value of a particular order parameter, the eigenvalue spectrum ceases to be real and the $\mathcal{PT}$-symmetric phase is broken spontaneously. This leads to a sudden change in the physical behavior of the system and is the main experimental signature of $\mathcal{PT}$-symmetric systems.

Although currently unobserved at a fundamental level, $\mathcal{PT}$-symmetric behavior has been simulated using classical optics. The optical diffraction equation under the paraxial approximation has the same form as the Schrödinger equation [4,5] and, hence, certain optical systems are able to exhibit many of the phenomenological features of quantum systems. For example, Ruther *et al.* [6,7] observed $\mathcal{PT}$-symmetric behavior in a system of parallel waveguides with balanced loss and gain. Here, the order parameter was the gain of the amplifying waveguide. Below threshold, the propagating light oscillated between the two waveguides as one would expect from a traditional directional coupler. Above threshold, the optical energy remained in the amplifying waveguide and the coupled mode oscillations vanished. Studies of $\mathcal{PT}$-symmetric optical systems have revealed a wealth of novel phenomena, including self-trapped solitons [8], coherent perfect absorption [9,10], unidirectional invisibility [11,12], and nonreciprocal light propagation [13].

Here, we consider whether the novel phenomenology of $\mathcal{PT}$-symmetric classical optics extends to quantum optical systems. One unique feature of quantum electrodynamics, the quantum field theory of electromagnetism, is the existence of vacuum fluctuations. Although the expectation value of the electric field operator in the vacuum vanishes, its variance is nonzero. Thus, at any point in time, the local electric field may be instantaneously finite. These fluctuations drive many nonclassical atomic processes such as Casimir-Polder shifts and spontaneous relaxation rates [14]. Control of these processes can be achieved by tailoring the vacuum fluctuations, which, in turn, can be performed by engineering the local environment of the atom [15]. A two-level atom in an optical cavity provides a classic example. If the atomic transition frequency is resonant with the cavity frequency, the atom's excited-state relaxation rate will be enhanced. Conversely, if frequency is off resonant with the cavity frequency, the relaxation rate will be suppressed. Such suppression of the relaxation rate cannot be achieved by direct repumping of the atom as the applied field will induce Rabi oscillations in the system driving the atom from the excited state back to the ground state. Hence, cavities and cavity quantum electrodynamics are critical tools in the control of atomic processes and, hence, play an important role in quantum control experiments. For example, magnetic atom chips will trap atoms in a specific Zeeman sublevel. Relaxation of the atom from the trapped state will result in an antitrapped state and the atom will be expelled from the trap [16–18]. Thus, to increase the trapping time, a crucial limiting factor for many quantum control experiments, suppression of the relaxation rate is highly desirable. Furthermore, the spontaneous relaxation rate is directly linked to the underlying vacuum fluctuations and hence acts as a probe of the nonclassical behavior of the vacuum. Thus, studies of this type will illuminate whether a $\mathcal{PT}$-symmetric environment can affect processes that are uniquely quantum mechanical.

*jac32@nyu.edu

Here, we study the spontaneous relaxation rate of a two-level atom in a $\mathcal{PT}$-symmetric cavity and compare the result to those of a usual $\mathcal{P}$-symmetric cavity. There have been a few studies of $\mathcal{PT}$-symmetric cavities before, e.g., Refs. [19,20], but these studies have been semiclassical in nature with a quantized two-level system and the cavity field treated classically. Here, we will treat the cavity in a fully quantum mechanical way to see whether $\mathcal{PT}$-symmetric effects are observable in quantum processes as well as in classical and semiclassical ones.

II. QUANTUM ELECTRODYNAMICS IN LINEARLY RESPONDING MEDIA

A. Absorbing media

The electric field modes $\mathbf{E}(\mathbf{r},\omega)$ in an absorbing medium obey the inhomogeneous Helmholtz equation

$$\nabla\times\boldsymbol{\mu}^{-1}(\mathbf{r},\omega)\nabla\times\mathbf{E}(\mathbf{r},\omega)-\frac{\omega^2}{c^2}\boldsymbol{\varepsilon}(\mathbf{r},\omega)\mathbf{E}(\mathbf{r},\omega)=i\omega\mu_0\mathbf{j}_N(\mathbf{r},\omega),\tag{1}$$

where $\boldsymbol{\varepsilon}(\mathbf{r},\omega)$ and $\boldsymbol{\mu}(\mathbf{r},\omega)$ are the electric permittivity and magnetic permeability tensors and

$$\mathbf{j}_N(\mathbf{r},\omega)=-i\omega\mathbf{P}_N(\mathbf{r},\omega)+\nabla\times\mathbf{M}_N(\mathbf{r},\omega)\tag{2}$$

is the noise current density, with $\mathbf{P}_N(\mathbf{r},\omega)$ and $\mathbf{M}_N(\mathbf{r},\omega)$ the noise polarization and noise magnetization fields, respectively [21,22]. The noise current density acts as a Langevin noise source which is related to the presence of absorption in the medium. The solutions to Eq. (1) are given by

$$\mathbf{E}(\mathbf{r},\omega)=i\omega\mu_0\int d^3r'\boldsymbol{G}(\mathbf{r},\mathbf{r}',\omega)\cdot\mathbf{j}_N(\mathbf{r}',\omega),\tag{3}$$

where $\boldsymbol{G}(\mathbf{r},\mathbf{r}',\omega)$ is the electromagnetic Green's function, which solves the Helmholtz equation for a point source [21–23]

$$\nabla\times\boldsymbol{\mu}^{-1}(\mathbf{r},\omega)\nabla\times\boldsymbol{G}(\mathbf{r},\mathbf{r}',\omega)-\frac{\omega^2}{c^2}\boldsymbol{\varepsilon}(\mathbf{r},\omega)\boldsymbol{G}(\mathbf{r},\mathbf{r}',\omega)=\delta(\mathbf{r}-\mathbf{r}').\tag{4}$$

These electric field modes can be quantized by relating the noise fields to a set of bosonic creation and annihilation operators $\hat{\mathbf{f}}_\lambda(\mathbf{r},\omega)$ ($\lambda\in e,m$), which obey the bosonic commutation relations

$$[\hat{\mathbf{f}}_\lambda(\mathbf{r},\omega),\hat{\mathbf{f}}^\dagger_{\lambda'}(\mathbf{r}',\omega')]=\delta_{\lambda\lambda'}\boldsymbol{\delta}(\mathbf{r}-\mathbf{r}')\delta(\omega-\omega'),\tag{5}$$

via the relations

$$\hat{\mathbf{P}}_{\mathrm{N}}(\mathbf{r},\omega)=i\sqrt{\frac{\hbar\varepsilon_0}{\pi}\mathrm{Im}\varepsilon(\mathbf{r},\omega)}\,\hat{\mathbf{f}}_e(\mathbf{r},\omega),\tag{6}$$

$$\hat{\mathbf{M}}_{\mathrm{N}}(\mathbf{r},\omega)=\sqrt{\frac{\hbar}{\mu_0\pi}\frac{\mathrm{Im}\mu(\mathbf{r},\omega)}{|\mu(\mathbf{r},\omega)|^2}}\,\hat{\mathbf{f}}_m(\mathbf{r},\omega).\tag{7}$$

Hence, one can express the quantized field electric modes as

$$\hat{\mathbf{E}}(\mathbf{r},\omega)=\sum_{\lambda=e,m}\int d^3r'\boldsymbol{G}_\lambda(\mathbf{r},\mathbf{r}',\omega)\cdot\hat{\mathbf{f}}_\lambda(\mathbf{r}',\omega),\tag{8}$$

where the coefficients $\boldsymbol{G}_\lambda(\mathbf{r},\mathbf{r}',\omega)$ are given by [21,22]

$$\boldsymbol{G}_e(\mathbf{r},\mathbf{r}',\omega)=i\frac{\omega^2}{c^2}\sqrt{\frac{\hbar}{\pi\varepsilon_0}\mathrm{Im}\varepsilon(\mathbf{r}',\omega)}\boldsymbol{G}(\mathbf{r},\mathbf{r}',\omega),\tag{9}$$

$$\boldsymbol{G}_m(\mathbf{r},\mathbf{r}',\omega)=-i\frac{\omega}{c}\sqrt{\frac{\hbar}{\pi\varepsilon_0}\frac{\mathrm{Im}\mu(\mathbf{r}',\omega)}{|\mu(\mathbf{r}',\omega)|^2}}[\boldsymbol{G}(\mathbf{r},\mathbf{r}',\omega)\times\overleftarrow{\nabla}'].\tag{10}$$

Note that the form of the noise fields is chosen such that the quantized field modes obey the fundamental field commutation relation

$$[\hat{\mathbf{E}}(\mathbf{r}),\hat{\mathbf{B}}(\mathbf{r}')]=-\frac{i\hbar}{\varepsilon_0}\nabla\times\delta(\mathbf{r}-\mathbf{r}').\tag{11}$$

B. Amplifying media

The extension of the above quantization scheme to amplifying media was performed in Ref. [24] and was used to study the impact of amplifying media on the Casimir force in Ref. [25]. The response of amplifying media can be characterized by a permittivity and a permeability with negative imaginary parts. The other major change to the formalism is that inside the amplifying medium, the roles of the creation and annihilation operators switch places [26]. Hence, the noise polarization operators take the form

$$\hat{\mathbf{P}}_{\mathrm{N}}(\mathbf{r},\omega)=i\sqrt{\frac{\hbar\varepsilon_0}{\pi}|\mathrm{Im}\varepsilon(\mathbf{r},\omega)|}\{\Theta[\mathrm{Im}\varepsilon(\mathbf{r},\omega)]\hat{\mathbf{f}}_e(\mathbf{r},\omega)+\Theta[-\mathrm{Im}\varepsilon(\mathbf{r},\omega)]\hat{\mathbf{f}}^\dagger_e(\mathbf{r},\omega)\},\tag{12}$$

$$\hat{\mathbf{M}}_{\mathrm{N}}(\mathbf{r},\omega)=\sqrt{\frac{\hbar}{\mu_0\pi}\frac{|\mathrm{Im}\mu(\mathbf{r},\omega)|}{|\mu(\mathbf{r},\omega)|^2}}\{\Theta[\mathrm{Im}\mu(\mathbf{r},\omega)]\hat{\mathbf{f}}_m(\mathbf{r},\omega)+\Theta[-\mathrm{Im}\mu(\mathbf{r},\omega)]\hat{\mathbf{f}}^\dagger_m(\mathbf{r},\omega)\},\tag{13}$$

where $\Theta[x]$ is the Heaviside step function.

This simple extension of the quantum electrodynamics formalism to amplifying media clearly has some limitations. The formalism assumes that the amplifying medium is in a quasistatic state. In practice, this requires the pumping of the amplifying medium to be sufficiently strong and the perturbations that are amplified to be sufficiently small that the proportion of excited atoms in the medium to remain approximately constant. This is valid for the study of dispersion forces as the photons involved in the interaction are (in principle) virtual and hence no real transitions take place in the medium. Similarly, with relaxation rates, the underlying interaction is with the virtual photons of the vacuum fluctuations, although in this case a real photon may be generated by the relaxing quantum system. In real systems, however, it is not possible to restrict all interaction as being purely virtual. In real gain media, real incoherent photons will be radiated either by spontaneous relaxation of the excited atoms or by a number of spontaneous amplification processes which result in a vacuum fluctuation resulting in the release of a real photon. In the following, we will neglect the effects of these real photons and concentrate on the vacuum effects that stem from the geometry of the system.

Here, we will study the relaxation of a single two-level atom in a $\mathcal{PT}$-symmetric cavity where one of the cavity walls is amplifying. Thus, the interaction of the atom with the amplifying cavity wall will be a virtual process. Furthermore, we assume that the number of excited atoms in the cavity wall is orders of magnitude greater than the single atom in the cavity and hence will only negligibly perturb the state of the amplifying cavity wall. Thus, the simple extension is sufficient for the purposes at hand.

III. SPONTANEOUS RELAXATION OF A TWO-LEVEL ATOM IN A CAVITY

Planar optical cavities with absorbing walls are traditionally modeled as a three-layered medium with a central vacuum region containing the atom bounded by infinitely thick material layers. In practice, the cavity walls will have a finite thickness but, if they are thick enough, any feedback from the outer interfaces of the cavity walls will have been damped away by the time it returns to the central vacuum region and hence will have negligible effect on the atom. For amplifying media, this may not be the case as feedback from the outer interfaces will be amplified by the wall rather than damped and hence may have a non-negligible effect on the atom. For this reason, we model the cavity as a five-layer medium.

Consider an atom in a planar cavity formed from a central vacuum region of width $L_3 = L_c$ with refractive index $n_3 = 1$, bounded by an absorbing medium of finite thickness $L_2 = L_w$ with refractive index $n_2 = n_r + in_i$ on the left and another medium also with finite thickness $L_4 = L_w$ (amplifying in a $\mathcal{PT}$-symmetric system or an absorbing in a $\mathcal{P}$-symmetric system) with refractive index $n_4 = n_r \pm in_i$ on the right. Note that for the system to be either $\mathcal{P}$- or $\mathcal{PT}$-symmetric the thickness of the cavity walls must be equal. The regions outside the cavity walls are also assumed to be vacuum with refractive index $n_1 = n_5 = 1$ (see Fig. 1). The origin of the coordinate system is taken to be at the center of the cavity.

The spontaneous relaxation rate for the atom in the cavity is given by [21]

$$\Gamma = \frac{2\pi}{\hbar^2}\mathbf{d}\cdot\langle 0|\hat{\mathbf{E}}^{\dagger}(\mathbf{r}_A,\omega_A)\hat{\mathbf{E}}(\mathbf{r}_A,\omega_A)|0\rangle\cdot\mathbf{d}, \tag{14}$$

where $\mathbf{d}$ is the dipole moment matrix element of the atomic transition and $\langle 0|\hat{\mathbf{E}}^{\dagger}(\mathbf{r}_A,\omega_A)\hat{\mathbf{E}}(\mathbf{r}_A,\omega_A)|0\rangle$ is the variance of the electric field mode operator in the vacuum at the location of the atom $\mathbf{r}_A$, with frequency equal to the atomic transition frequency ω_A. Expanding the electric field modes using Eq. (8) for the case of a spherically averaged atomic dipole (i.e., the dipole moment of the atom is not aligned in any specific direction), the spontaneous relaxation rate reduces to [21,27]

$$\Gamma = A_0\{\mathrm{Tr}[\mathrm{Im}G_0(\mathbf{r}_A,\mathbf{r}_A,\omega_A)] + \mathrm{Tr}[\mathrm{Im}G_S(\mathbf{r}_A,\mathbf{r}_A,\omega_A)]\}, \tag{15}$$

where $A_0 = 2\omega_A^2|\mathbf{d}|^2/3\hbar\epsilon_0 c^2$ is a constant that contains the details of the atomic transition. The first term in Eq. (15), which is proportional to the vacuum Green's function $G_0(\mathbf{r}_A,\mathbf{r}_A,\omega_A)$, the solution to Eq. (4) in the vacuum, gives the free-space relaxation rate Γ_0. The second term in Eq. (15), which is proportional to the scattering Green's function $G_S(\mathbf{r}_A,\mathbf{r}_A,\omega_A)$, the solution to Eq. (4) for electromagnetic waves scattered by the cavity walls, gives the surface-induced relaxation rate Γ_S, which is the change in relaxation rate owing to the presence of the cavity.

It is worth briefly commenting on the sign of Γ. In Eq. (14), one has implicitly assumed that the atomic frequency ω_A is positive (i.e., the transition is from a higher-energy state to a lower-energy state). However, it is possible for the atom to be driven from a lower-energy state to a higher-energy state. This can happen, for example, in a finite-temperature environment when thermal photons can drive upward transitions. In such cases, ω_A is negative and one obtains an overall minus sign for the relaxation rate. Hence, negative relaxation rates indicate a situation where the atom is being driven from the ground state to the excited state. If one solves the optical Bloch equations in the interaction picture for the atom with a positive relaxation rate and the constraints that the atomic populations cannot exceed unity, $\sigma_g \leqslant 1$, $\sigma_e \leqslant 1$ and that the total population must always be unity, $\sigma_g + \sigma_e = 1$, one obtains

$$\sigma_g = 1 - \sigma_{e,0}e^{-\Gamma t}, \tag{16}$$

$$\sigma_e = \sigma_{e,0}e^{-\Gamma t}. \tag{17}$$

Here, as $t \to \infty$, the population relaxes to the ground state. When one has a negative relaxation rate, the roles of the ground and excited states swap and, hence, one finds

$$\sigma_g = \sigma_{g,0}e^{-\Gamma t}, \tag{18}$$

$$\sigma_e = 1 - \sigma_{g,0}e^{-\Gamma t}, \tag{19}$$

and, as $t \to \infty$, the population relaxes to the excited state.

Using the expression for the appropriate Green's function, one finds that the spontaneous relaxation rate for a planar cavity reduces to [22,23]

$$\Gamma_S = \frac{A_0}{4\pi}\mathrm{Re}\left\{\int_0^{\infty} dk_{\parallel}\frac{k_{\parallel}}{k_{z,2}}\left[F^s + \left(\frac{2k_{\parallel}^2}{k_2^2} - 1\right)F^p\right]\right\}, \tag{20}$$

where $k_i = \omega n_i/c$, $k_{\parallel}$ is the transverse part of the wave vector, $k_{z,i} = \sqrt{k_i^2 - k_{\parallel}^2}$, and

$$F^{\alpha} = [R_-^{\alpha}e^{-ik_{z,2}(2z-L_c)} + R_+^{\alpha}e^{ik_{z,2}(2z+L_c)} + 2R_-^{\alpha}R_+^{\alpha}e^{2ik_{z,2}L_c}]M_3^{\alpha} \tag{21}$$

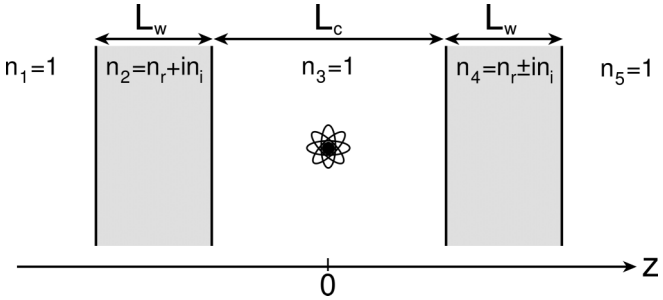

FIG. 1. Schematic of the planar cavity. Region 2 is absorbing, whereas region 4 is absorbing for the $\mathcal{P}$ symmetry and amplifying for $\mathcal{PT}$ symmetry. Regions 1, 3, and 5 constitute the vacuum.

with the generalized multilayer reflection coefficients $R^{\alpha}_{\pm}$ at the $L_c/2$ and $-L_c/2$ boundaries reading as [23]

$$R^{\alpha}_{+} = R^{\alpha}_{34} + T^{\alpha}_{34} R^{\alpha}_{45} T^{\alpha}_{43} M^{\alpha}_{4} e^{2ik_{z,4}L_4}, \tag{22}$$

$$R^{\alpha}_{-} = R^{\alpha}_{32} + T^{\alpha}_{32} R^{\alpha}_{21} T^{\alpha}_{23} M^{\alpha}_{2} e^{2ik_{z,2}L_2}, \tag{23}$$

with single-layer coefficients given by

$$R^{s}_{ij} = \frac{k_{z,i} - k_{z,j}}{k_{z,i} + k_{z,j}}, \quad R^{p}_{ij} = \frac{n_j^2 k_{z,i} - n_i^2 k_{z,j}}{n_j^2 k_{z,i} + n_i^2 k_{z,j}}, \tag{24}$$

$$T^{s}_{ij} = \frac{2k_{z,i}}{k_{z,i} + k_{z,j}}, \quad T^{p}_{ij} = \frac{2n_j^2 k_{z,i}}{n_j^2 k_{z,i} + n_i^2 k_{z,j}}, \tag{25}$$

and multiple reflection coefficients given by

$$M^{\alpha}_{i} = \left[1 - R^{\alpha}_{i,i+1} R^{\alpha}_{i,i-1} e^{2ik_{z,i}L_i}\right]^{-1}. \tag{26}$$

The superscript α indicates the s (TE) and p (TM) polarizations, respectively. It should be noted that the expression in Eq. (20) coincides with that for classical dipole radiation in a planar cavity as found previously in Refs. [28–31].

IV. EVALUATION OF THE $k_{\parallel}$ INTEGRAL

To obtain an expression for the spontaneous relaxation rate, one needs to perform the integral over the transverse part of the wave vector in Eq. (20). For amplifying media, care must be taken. The electric permittivity takes the form of a Lorentzian response function and hence has poles in the complex plane. As discussed by Skaar [32–34], to obtain a physically valid result one must integrate along the branch of the complex plane that lies above these poles. For absorbing media, the poles lie below the real axis and one can integrate along the real axis in a straightforward way. For amplifying media, the poles lie above the real axis and, hence, one must deform the contour of integration so it passes above them. This leads to a contour along which $\mathrm{Im}[k_z] > 0$ for $k_{\parallel} > \omega\sqrt{\epsilon}/c$ and, hence, the evanescent waves decay away. The physical interpretation for this relates to the mechanism by which gain is generated in the amplifying medium. Gain is achieved by creating a population inversion of a particular atomic transition with amplification achieved via stimulated emission. The evanescent field can cause stimulated emission, but the released photon is a propagating one. Therefore, in the presence of an evanescent field, the medium amplifies the associated propagating mode rather than the evanescent field itself and, hence, the evanescent field should still decay into the amplifying medium.

The deformed contour also has an extra contribution from the pole itself. This contribution is divergent. This divergence is an artifact of the idealized nature of the system and stems from the wave vector at $k_z = 0$. This wave propagates along the surface of the amplifying material and, as the material is both unbounded in the transverse direction and does not feature gain saturation, leads to infinite amplification. In a real physical system the boundedness of the cavity wall and the ability of the gain to saturate will mean that this contribution will not actually diverge. However, as this mode is traveling in the transverse direction and not into the cavity, it will have a minimal influence on the atom. Hence, this contribution is negligible.

A further issue with the evaluation of the transverse wave-vector integral relates to the interpretation of the multiple reflection coefficient M^{α}_{i} in amplifying media. The traditional interpretation of M^{α}_{i} can be seen by expanding it as a Taylor series

$$\left[1 - R^{\alpha}_{i,i+1} R^{\alpha}_{i,i-1} e^{2ik_{z,i}L_i}\right]^{-1} = 1 + R^{\alpha}_{i,i+1} R^{\alpha}_{i,i-1} e^{2ik_{z,i}L_i} + R^{\alpha}_{i,i+1} R^{\alpha}_{i,i-1} e^{2ik_{z,i}L_i} R^{\alpha}_{i,i+1} R^{\alpha}_{i,i-1} e^{2ik_{z,i}L_i} + \cdots. \tag{27}$$

Each term relates to an optical path that scatters off a certain number of interfaces before being transmitted out of the slab. In absorbing media, owing to the positive imaginary part of the refractive index, the exponential factor decays away and, hence,

$$R^{\alpha}_{i,i+1} R^{\alpha}_{i,i-1} e^{2ik_{z,i}L_i} < 1. \tag{28}$$

Thus, the series always converges. In amplifying media, the negative imaginary part of the refractive index causes the exponential factor to grow and, if the gain is large enough and the reflection coefficients are close enough to unity, then

$$R^{\alpha}_{i,i+1} R^{\alpha}_{i,i-1} e^{2ik_{z,i}L_i} > 1. \tag{29}$$

In this case, although the closed-form expression for M^{α}_{i} is finite, the series does not converge. The last case is where

$$R^{\alpha}_{i,i+1} R^{\alpha}_{i,i-1} e^{2ik_{z,i}L_i} = 1. \tag{30}$$

Here, both the closed-form expression and series expansion of M^{α}_{i} diverge. This last case is the point where the gain is sufficiently large that the amplitude of the electromagnetic wave returns to the same value after one round trip despite losses owing to transmission through the interfaces. This marks the onset of lasing and is known as the lasing threshold.

There is still some debate about how to interpret M^{α}_{i} above the lasing threshold. Certain authors have stated that although the series diverges, the closed-form expression for M^{α}_{i} is still valid [35], while others state that it is not [36]. Others have suggested that convergence of the series can come from inversion of the Poynting vector [37] or have proposed upper bounds to the reflection coefficients [38]. Physically, any amplifying medium will be subject to gain saturation at very high field amplitudes owing to the inability to maintain the population inversion. Gain saturation is a nonlinear effect which is not included in the simple model of amplifying media used here. Furthermore, such a situation violates the assumption that the amplifying medium is quasistatic, an assumption that was used to formulate the quantum electrodynamical field theory in amplifying media in Sec. II B. For this reason, we will restrict ourselves to gains below the lasing threshold where both the closed form and series expansion of M^{α}_{i} are valid.

V. ASYMPTOTIC SOLUTIONS

The integral in Eq. (20) can be split into two parts. In the interval $0 < k_\parallel \leqslant k_i$, $k_{z,i}$ is real. This describes a propagating field. In the interval $k_i < k_\parallel \leqslant \infty$, $k_{z,i}$ is imaginary. This describes an evanescent field. Thus, the total relaxation rate is the sum of three contributions: the propagating part and the evanescent part of the scattering relaxation rate, which originates from the second term in Eq. (15), and the free-space relaxation rate, which originates from the first term in Eq. (15). In general, one cannot solve the integral in Eq. (20) analytically. However, in certain limits one can obtain analytical approximations that are useful in illuminating the asymptotic physics of the system.

A. Large cavities

For large cavities, where the distance from the atom to the cavity wall is $z \gg c/\omega_A$, one can integrate the Green's function using the method of stationary phase. In this approximation, only the propagating part of the integral is computed and the evanescent part neglected. At the stationary phase point at $k_\parallel = 0$, $k_{z,i} \to k_i = \omega n_i/c$ and the single-layer reflection and transmission coefficients simplify to

$$R^s_{ij} \approx \frac{n_i - n_j}{n_i + n_j}, \quad R^p_{ij} \approx \frac{n_j - n_i}{n_i + n_j}, \tag{31}$$

$$T^s_{ij} \approx \frac{2n_i}{n_i + n_j}, \quad T^p_{ij} \approx \frac{2n_j}{n_i + n_j}, \tag{32}$$

and

$$M^\alpha_i \approx \left[1 - R^\alpha_{i,i+1} R^\alpha_{i,i-1} e^{2ik_i L_i}\right]^{-1}. \tag{33}$$

This leads to

$$R^s_- = -R^p_- = \frac{\left(1 - n_2^2\right)\sin[k_2 L_w]}{2in_2\cos[k_2 L_w] + \left(1 + n_2^2\right)\sin[k_2 L_w]}, \tag{34}$$

$$R^s_+ = -R^p_+ = \frac{\left(1 - n_4^2\right)\sin[k_4 L_w]}{2in_4\cos[k_4 L_w] + \left(1 + n_4^2\right)\sin[k_4 L_w]}. \tag{35}$$

Integrating the exponential factors of the Green's function to leading order in z leads to

$$\Gamma_S = A_0 \frac{|M_3|}{2\pi}\left[|R_-|\frac{\sin\left[\frac{\omega}{c}(2z - L_c) - \theta_- - \theta_{M_3}\right]}{(2z - L_c)} + |R_+|\frac{\sin\left[\frac{\omega}{c}(2z + L_c) + \theta_+ + \theta_{M_3}\right]}{(2z + L_c)}\right], \tag{36}$$

where $|R_\pm|$ and $\theta_\pm$ are the magnitude and argument of the generalized reflection coefficients and $|M_3|$ and θ_{M_3} are the magnitude and argument of the multiple scattering coefficient within the cavity. For a $\mathcal{P}$-symmetric cavity $|R_+| = |R_-|$ and $\theta_+ = \theta_-$ whereas in a $\mathcal{PT}$-symmetric cavity $|R_+| = |R_-|$ and $\theta_+ = -\theta_-$. Thus, the difference between the two cavities is limited to a slight suppression of the relaxation rate owing to the change in the interference between the two terms in Eq. (36).

B. Small cavities

For small cavities, where the distance from the atom to the cavity wall is $z \ll c/\omega_A$, one can expand k_z as

$$k_{z,i} = \sqrt{k_i^2 - k_\parallel^2} \approx ik_\parallel + O\left(\frac{k_i^2}{2k_\parallel^2}\right). \tag{37}$$

This approximation only computes the evanescent part of the integral and the propagating part is neglected. In this case, single-layer reflection and transmission coefficients simplify to

$$R^s_{ij} \approx 0, \quad R^p_{ij} \approx \frac{n_j^2 - n_i^2}{n_i^2 + n_j^2}, \tag{38}$$

$$T^s_{ij} \approx 1, \quad T^p_{ij} \approx \frac{2n_j^2}{n_i^2 + n_j^2}, \tag{39}$$

and

$$M^\alpha_i \approx \left[1 - R^\alpha_{i,i+1} R^\alpha_{i,i-1} e^{-2k_\parallel L_i}\right]^{-1}. \tag{40}$$

This leads to

$$R^p_- = \frac{\left(1 - n_2^4\right)\sinh[k_2 L_w]}{2n_2^2\cosh[k_2 L_w] + \left(1 + n_2^4\right)\sinh[k_2 L_w]}, \tag{41}$$

$$R^p_+ = \frac{\left(1 - n_4^4\right)\sinh[k_4 L_w]}{2n_4^2\cosh[k_4 L_w] + \left(1 + n_4^4\right)\sinh[k_4 L_w]}, \tag{42}$$

and $R^s_+ = R^s_- = 0$. Treating the approximate generalized reflection coefficients above as complex numbers with a magnitude and an argument and expanding the multiple reflection coefficient in the cavity M_3^p as an infinite series and integrating each term to leading order in $k_\parallel$ leads to

$$\Gamma_S = A_0 \frac{c^2}{\pi\omega^2}\sum_{j=0}^{\infty}\left\{|R_+|^j|R_-|^{j+1}\frac{\sin[j\theta_+ + (j+1)\theta_-]}{[(2j+1)L_c - 2z]^3} + |R_+|^{j+1}|R_-|^j\frac{\sin[(j+1)\theta_+ + j\theta_-]}{[(2j+1)L_c + 2z]^3}\right\}. \tag{43}$$

As $|R_+| = |R_-|$ and $\theta_+ = -\theta_-$ in the $\mathcal{PT}$-symmetric case, the evanescent contribution to the relaxation rate vanishes identically at the cavity center ($z = 0$). Thus, the main contribution to the relaxation rate in small cavities is completely suppressed. The reason for the suppression is that the phase shift of the reflected wave at each end of a $\mathcal{PT}$-symmetric cavity is equal and opposite and, hence, there is complete destructive interference of the reflected waves at the center of the cavity.

VI. NUMERICAL RESULTS

Experimental realization of $\mathcal{PT}$-symmetric classical optical systems has already been achieved using iron-doped lithium niobate waveguides [6]. The system was driven by an Ar^+ laser at 514.5 nm. Absorption in the system was provided by iron dopants and the gain by a two-wave mixing process in the lithium niobate driven by a separate pump beam [39–41]. This allowed the absorption and gain parameters to be varied by changing the iron dopant concentration and pump beam intensity, respectively. A similar setup can be used

to create a $\mathcal{PT}$-symmetric planar cavity with a pump beam providing gain for one of the cavity walls and iron doping enhancing the absorption of the other. The active frequency of this cavity (514.5 nm) is close to the magnesium $3s4s \rightarrow 3s3p$ transition frequencies, 516.7 nm, 516.3 nm, 518.4 nm for the final-state angular momentum of $J = 0$, 1, and 2, respectively, and, hence, one would be able to observe the $\mathcal{PT}$-symmetric properties of the cavity with this atom. The three magnesium $3s4s \rightarrow 3s3p$ lines are all persistent with relative intensities of 12, 40, and 70 compared to 1000 for the brightest transition ($3s^2 \rightarrow 3s3p$), and are comparable to the second brightest persistent line which has a relative brightness of 80 ($3s4p \rightarrow 3s3d$) [42]. Furthermore, magnesium atoms have been successfully trapped using magneto-optical traps [43,44].

Using the above parameters with $n_r = 2.33$ (the refractive index of lithium niobate at 514.5 nm), we numerically integrate the Green's function to find the spontaneous relaxation rate within a $\mathcal{P}$- or $\mathcal{PT}$-symmetric cavity. For the wall thickness we use $L_w = 1000\lambda$ where λ is the vacuum wavelength. The Lasing threshold can be estimated from [45]

$$n_i \approx \frac{\lambda}{4\pi L_w} \ln R_+ R_-, \tag{44}$$

which for the parameters above is on the order of $n_i \approx 10^{-4}$. Far below the lasing threshold, the wall thickness L_w only weakly affects the relaxation rate as the propagation excitation that propagates through is not sufficiently amplified for any reflection from the outer interface of the cavity wall to have a strong effect. As one approaches the lasing threshold, the cavity wall thickness begins to have a stronger effect on the relaxation rate. However, as previously discussed in Sec. IV, as one approaches the lasing threshold the simplified description of the gain medium becomes less accurate and, hence, any result taken in this regime must be interpreted with care.

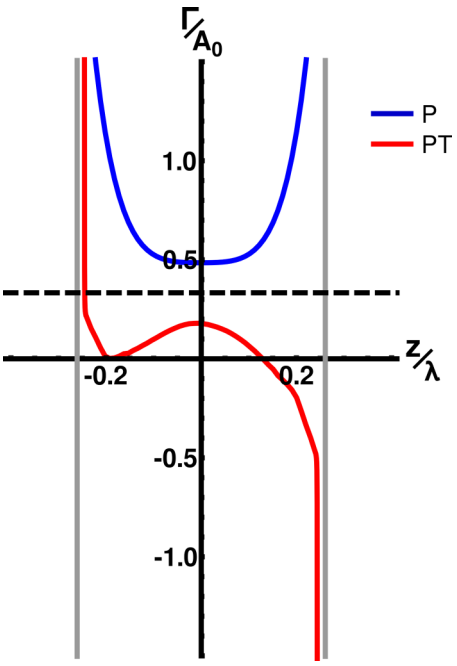

FIG. 2. The spontaneous relaxation rate in $\mathcal{P}$- (blue) and $\mathcal{PT}$- (red) symmetric cavity. Here, $n_2 = n_4 = 2.33 + 10^{-6}i$ and $n_2 = n_4^* = 2.33 + 10^{-6}i$ for the $\mathcal{P}$- and $\mathcal{PT}$-symmetric cavities, respectively. The width of the cavity is $L_c = \lambda/2$. The vertical gray lines indicate the location of the cavity walls and the horizontal black dashed line indicates the free-space relaxation rate.

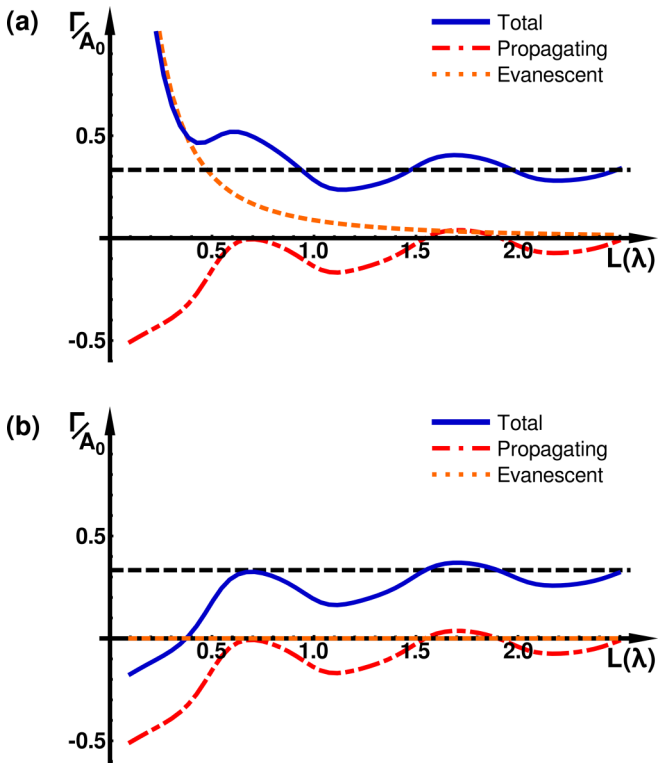

FIG. 3. The spontaneous relaxation rate at the center of the cavity for (a) $\mathcal{P}$-symmetric cavity with $n_2 = n_4 = 2.33 + 10^{-6}i$, and (b) $\mathcal{PT}$-symmetric cavity with $n_2 = n_4^* = 2.33 + 10^{-6}i$. The horizontal black dashed line is the free-space relaxation rate.

Figure 2 shows the spontaneous relaxation rate for a planar microcavity with width $L_c = \lambda/2$ and an absorptionor gain coefficient of $n_i = 10^{-6}$. For the $\mathcal{P}$-symmetric cavity, the spontaneous relaxation rate increases as the atom nears the walls. This is owing to the increase in the nonradiative decay to the absorption modes in the material. Hence, the presence of absorbing cavity walls leads to short excited-state lifetimes. In the $\mathcal{PT}$-symmetric cavity, close to the gain medium the spontaneous relaxation becomes negative. As discussed in Sec. III, this implies that the atom is pumped by the amplified field, leading to upward atomic transitions. The phase shifts of the evanescent field reflected from the gain and absorbing media are equal and opposite and so destructively interfere near the center of the cavity.

Figure 3 shows the variation in the spontaneous relaxation rate at the center of the cavity as a function of cavity width for the $\mathcal{P}$-symmetric [Fig. 3(a)] and $\mathcal{PT}$-symmetric [Fig. 3(b)] cavities. The important detail to note is that, for the $\mathcal{P}$-symmetric cavity, the evanescent contribution to the spontaneous relaxation rate increases as the cavity width decreases and, for cavities smaller than a wavelength, is the dominant relaxation pathway. For a $\mathcal{PT}$-symmetric cavity, the

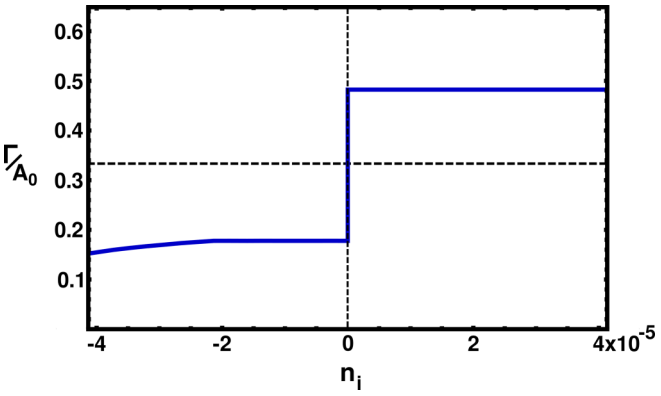

FIG. 4. The spontaneous relaxation rate at the center of the cavity as a function of n_i. Here, $n_{2r} = n_{4r} = 2.33$ and $n_{2i} = |n_{4i}|$. The width of the cavity is $L = \lambda/2$. The horizontal black dashed line is the free-space relaxation rate.

evanescent contribution vanishes for all cavity widths. Hence, the major contribution to the spontaneous relaxation rate in small cavities is completely suppressed.

Figure 4 shows the spontaneous relaxation rate at the center of the microcavity with width $L_c = \lambda/2$ as a function of the gain or absorption parameter, $n_i = \mathrm{Im}[n_4]$, of the right-hand cavity wall. At $n_i = 0$, there is a sudden change in the spontaneous relaxation rate as the system changes from a $\mathcal{PT}$-symmetric system to $\mathcal{P}$-symmetric system. Although this distinct change in the phenomenology of the cavity is not caused by a $\mathcal{PT}$-phase transition (the $\mathcal{PT}$ phase is not broken spontaneously at $n_i = 0$, $\mathcal{T}$ symmetry is broken explicitly), it shows a sharp phenomenological change in the behavior of the system and distinguishes the $\mathcal{P}$- and $\mathcal{PT}$-symmetric cavities and would be a distinct experimental signature.

The reason for the sudden discontinuity, rather than a smooth transition, is the sudden breaking of $\mathcal{T}$ symmetry at $n_i = 0$. In the $\mathcal{PT}$-symmetric regime, the phase shift at each side of the cavity is always equal and opposite for all $n_i < 0$ and, hence, the vacuum fluctuations undergo destructive interference at the center of the cavity and the evanescent contribution of the relaxation rate vanishes. At $n_i = 0$, $\mathcal{T}$ symmetry is broken and in the P-symmetric regime the phase shift at each side of the cavity is equal for all $n_i > 0$ and, hence, the vacuum fluctuations at the center of the cavity experience a change from destructive interference to constructive interference and one observes a discontinuous jump in the relaxation rate. It is important to note that the real part of the refractive index is not changing so the relaxation rate will not go smoothly to zero (the cavity does not vanish, only the gain or loss characteristics change). One can see this phenomenology in Eq. (43) where, at the center of the cavity, the expression reduces to a pair of Fourier sine series which describe a sudden step transition at $n_i = 0$.

VII. SUMMARY

Here, we have shown that a $\mathcal{PT}$-symmetric planar cavity is able to suppress the spontaneous relaxation rate of a two-level atom below the vacuum level. Suppression of the spontaneous relaxation rate is useful in many areas of quantum control where increase of the excited-state lifetime is required. Such situations include atom traps where only specific states are trapped or quantum computation applications where maintaining the excited states is required for the realization of long-lasting qubits.

[1] C. M. Bender and S. Boettcher, Phys. Rev. Lett. **80**, 5243 (1998).
[2] C. M. Bender, D. C. Brody, and H. F. Jones, Phys. Rev. Lett. **89**, 270401 (2002).
[3] C. M. Bender, D. C. Brody, H. F. Jones, and B. K. Meister, Phys. Rev. Lett. **98**, 040403 (2007).
[4] A. Yariv, *Optical Electronics in Modern Communications* (Oxford University Press, Oxford, 1997).
[5] P. Yeh, *Introduction to Photorefractive Nonlinear Optics*, Wiley Series in Pure and Applied Optics (Wiley, New York, 2001).
[6] C. E. Ruter, K. G. Makris, R. El-Ganainy, D. N. Christodoulides, M. Segev, and D. Kip, Nat. Phys. **6**, 192 (2010).
[7] L. Feng, R. El-Ganainy, and L. Ge, Nat. Photonics **11**, 752 (2017).
[8] Z. H. Musslimani, K. G. Makris, R. El-Ganainy, and D. N. Christodoulides, Phys. Rev. Lett. **100**, 030402 (2008).
[9] S. Longhi, Phys. Rev. A **82**, 031801(R) (2010).
[10] Y. D. Chong, L. Ge, and A. D. Stone, Phys. Rev. Lett. **106**, 093902 (2011).
[11] Z. Lin, H. Ramezani, T. Eichelkraut, T. Kottos, H. Cao, and D. N. Christodoulides, Phys. Rev. Lett. **106**, 213901 (2011).
[12] A. Regensburger, C. Bersch, M.-A. Miri, G. Onishchukov, D. N. Christodoulides, and U. Peschel, Nature (London) **488**, 167 (2012).
[13] L. Feng, M. Ayache, J. Huang, Y.-L. Xu, M.-H. Lu, Y.-F. Chen, Y. Fainman, and A. Scherer, Science **333**, 729 (2011).
[14] P. W. Milloni, *The Quantum Vacuum* (Academic, New York, 1994).
[15] E. M. Purcell, Phys. Rev. **69**, 681 (1946).
[16] M. P. A. Jones, C. J. Vale, D. Sahagun, B. V. Hall, and E. A. Hinds, Phys. Rev. Lett. **91**, 080401 (2003).
[17] P. K. Rekdal, S. Scheel, P. L. Knight, and E. A. Hinds, Phys. Rev. A **70**, 013811 (2004).
[18] R. Fermani, S. Scheel, and P. L. Knight, Phys. Rev. A **73**, 032902 (2006).
[19] Z.-P. Liu, J. Zhang, S. K. Özdemir, B. Peng, H. Jing, X.-Y. Lu, C.-W. Li, L. Yang, F. Nori, and Y.-X. Liu, Phys. Rev. Lett. **117**, 110802 (2016)
[20] S. Longhi, Europhys. Lett. **115**, 61001 (2016).
[21] S. Scheel and S. Y. Buhmann, Acta Phys. Slov. **58**, 675 (2008).
[22] S. Y. Buhmann, *Dispersion Forces I* (Springer, Berlin, 2012).
[23] W. C. Chew, *Waves and Fields in Inhomogeneous Media* (IEEE Press, Piscataway, NJ, 1995).

[24] C. Raabe and D.-G. Welsch, Eur. Phys. J. Special Topics **160**, 371 (2008).
[25] A. Sambale, S. Y. Buhmann, H. T. Dung, and D.-G. Welsch, Phys. Rev. A **80**, 051801(R) (2009).
[26] L. Knöll, S. Scheel, and D.-G. Welsch, QED in dispersing and absorbing media, in *Coherence and Statistics of Photons and Atoms*, edited by J. Peřina (Wiley, New York, 2001), pp. 1–63.
[27] J. A. Crosse and S. Scheel, Phys. Rev. A **79**, 062902 (2009).
[28] R. R. Chance, A. Prock, and R. Silbey, J. Chem. Phys. **62**, 2245 (1975).
[29] R. R. Chance, A. Prock, and R. Silbey, Adv. Chem. Phys. **37**, 1 (1978).
[30] J. M. Wylie and J. E. Sipe, Phys. Rev. A **30**, 1185 (1984).
[31] J. M. Wylie and J. E. Sipe, Phys. Rev. A **32**, 2030 (1985).
[32] J. Skaar, Phys. Rev. E **73**, 026605 (2006).
[33] J. Skaar, Opt. Lett. **31**, 3372 (2006).
[34] B. Nistad and J. Skaar, Phys. Rev. E **78**, 036603 (2008).
[35] J. C. J. Paasschens, T. Sh. Misirpashaev, and C. W. J. Beenakker, Phys. Rev. B **54**, 11887 (1996).
[36] X. Jiang, Q. Li, and C. M. Soukoulis, Phys. Rev. B **59**, R9007 (1999).
[37] T. S. Mansuripur and M. Mansuripur, Appl. Phys. Lett. **104**, 121106 (2014).
[38] R. V. Karapetyan, Laser. Phys. **17**, 1053 (2007).
[39] P. Yeh, IEEE J. Quantum Electron. **25**, 484 (1989).
[40] J. H. Hong, A. E. Chiou, and P. Yeh, Appl. Opt. **29**, 3026 (1990).
[41] J. P. Huignard and A. Marrakchi, Opt. Commun. **38**, 249 (1981).
[42] J. E. Sansonetti and W. C. Martin, *Handbook of Basic Atomic Spectroscopic Data* (AIP, New York, 2005).
[43] F. Y. Loo, A. Brusch, S. Sauge, M. Allegrini, E. Arimondo, N. Andersen, and J. W. Thomsen, J. Opt. B: Quantum Semiclass. Opt. **6**, 81 (2004).
[44] A. N. Goncharov, A. E. Bonert, D. V. Brazhnikov, A. M. Shilov, and S. N. Bagayev, Quantum Electron. **44**, 521 (2014).
[45] K. Thyagarajan and A. Ghatak, *Lasers: Fundementals and Applications, 2nd Ed.* (Springer, New York, 2010).